J. of Electromagn. Waves and Appl., Vol. 17, No. 7, 989–1008, 2003

A MARKOVIAN REGULARIZATION APPROACH OF THE MODIFIED GRADIENT METHOD FOR SOLVING A TWO-DIMENSIONAL INVERSE SCATTERING PROBLEM

A. Baussard

SATIE, UMR-CNRS 8029, ENS de Cachan
61 Avenue du Président Wilson, 94235 Cachan Cedex, France

K. Belkebir

Institut Fresnel, UMR-CNRS 6133
Campus de Saint Jérôme, Case 162, 13397 Marseille Cedex 20, France

D. Prémel

SATIE, UMR-CNRS 8029, ENS de Cachan
61 Avenue du Président Wilson, 94235 Cachan Cedex, France

Abstract—In this paper, we consider a two-dimensional inverse scattering problem dealing with microwave tomography. To solve this non-linear and ill-posed problem, an iterative scheme based on the Modified Gradient Method (MGM) is used. A Bayesian estimation framework was chosen to build up a regularization scheme based on the weak membrane model. The object to be retrieved being represented by a complex function, two energy terms acting separately on the real and imaginary parts were considered. Consequently, some modifications of the MGM were done. The resulting algorithm is tested against microwave laboratory-controlled data.

1. INTRODUCTION

Various applications are concerned with determining the location and the spatial variation of some physical proprieties of an object from measurements of the scattered response to a known electromagnetic or acoustic excitation. For example, in microwave imaging, the goal is to reconstruct the complex permittivity distribution of an object. Several algorithms have been developed to solve this inverse scattering problem. First algorithms dealt with linear inverse problems, and were based on diffraction tomography [8, 15], which is a generalization of classical X-ray computer tomography by taking into account diffraction effects. These algorithms provide an almost real-time approximate reconstructions of the polarization current density distribution, and, under the Born approximation, of the complex permittivity distribution. The limitation of diffraction tomography (essentially weak scatterers) stimulated the recent development of iterative methods [7, 9, 10, 16] for complex permittivity reconstruction of highly contrasted objects. These iterative methods deal with the nonlinearity of the inverse scattering problem and are, therefore, computationally more intensive. They are also more sensitive to ill-posedness of the inverse problem, which demand some *a priori* information.

In the present paper, the authors restrict the study to an iterative scheme based on the modified gradient method (MGM) introduced by Kleinman and van den Berg [10]. It consists in updating simultaneously, for each iteration step, the unknown field

in the scattering domain and the unknown constitutive material by minimizing a cost functional. This cost functional is composed of two normalized errors satisfying the field equation and matching the measured data. Some modifications of the MGM formulation have been done in order to take into account that the object to be reconstructed is complex. Moreover, a regularization scheme is built up, within the Bayesian estimation framework, to enhance the obtained reconstruction. This leads to introducing *a priori* information on the object by adding a regularizing functional. In [17], an additive Total Variation (TV) regularization procedure was incorporated in the MGM. The reported results clearly showed significant improvements in the reconstruction. Here, the authors investigate the possibility of a Markovian regularization scheme based on the weak membrane model [5] to regularize the MGM. This regularization has already been successfully used for solving inverse linear problems [12, 18], and for a non-linear inverse scattering problem [2] using a particular scheme based on the conjugate gradient approach.

Taking advantage of the proposed MGM formulation, two regularization functionals acting respectively on the real and imaginary parts of the object are considered. To test this regularized MGM and to show the interest of this approach, some results using real data are presented.

The paper is organized as follows. In Section 2, the statement of the problem is presented. Section 3 presents the proposed new MGM formulation and in Section 4, a Bayesian estimation framework of the joint estimation is considered in order to introduce *a priori* knowledge and define a regularized solution. Section 5 describes the regularized modified gradient method and the considered regularizing energy. In Section 6, the proposed algorithm is tested against real data. Finally, Section 7 gives some concluding remarks.

2. FORMULATION OF THE PROBLEM

The geometry of the problem studied in this paper is as depicted in Figure 1 where a two-dimensional object of arbitrary cross-section Ω_o is confined in a bounded domain Ω. The embedding medium Ω_b is assumed to be infinite and homogeneous, with permittivity $\varepsilon_b = \varepsilon_0\varepsilon_{br}$, and of permeability $\mu = \mu_0$ (ε_0 and μ_0 being the permittivity and permeability of the vacuum, respectively). The scatterers are assumed to be inhomogeneous dielectric and/or conductive cylinders with complex permittivity distribution $\varepsilon(\mathbf{r}) = \varepsilon_0\varepsilon_r(\mathbf{r})$; the entire configuration is non-magnetic ($\mu = \mu_0$).

A right-handed Cartesian coordinate frame $(O, \mathbf{u}_x, \mathbf{u}_y, \mathbf{u}_z)$ is

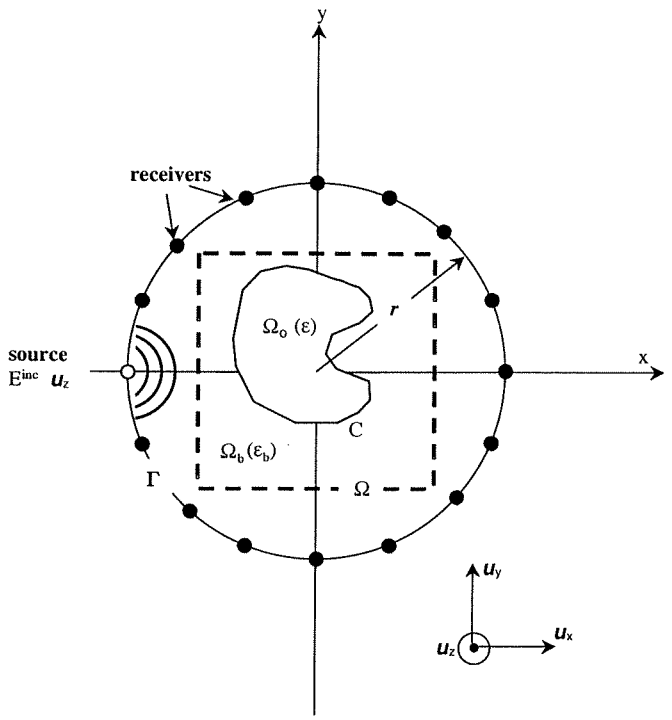

Figure 1. Geometry of the studied problem.

defined. The origin O can be either inside or outside the scatterer and the z-axis is parallel to the invariance axis of the scatterer. Then, the position vector OM can be written as:

$$OM = x\mathbf{u}_x + y\mathbf{u}_y + z\mathbf{u}_z = \mathbf{r} + z\mathbf{u}_z. \tag{1}$$

The sources that generate the electromagnetic excitation are assumed to be lines parallel to the z-axis, located at $(\mathbf{r}_l)_{1\leq l\leq L}$. Taking into account a time factor $\exp(-i\omega t)$, in the TM case (Transverse Magnetic case) the time-harmonic incident electric field created by the l^{th} line source is given by:

$$\mathbf{E}_l^{inc}(\mathbf{r}) = E_l^{inc}(\mathbf{r})\mathbf{u}_z = P\frac{\omega\mu_0}{4}H_0^{(1)}(k_b|\mathbf{r}-\mathbf{r}_l|)\mathbf{u}_z, \tag{2}$$

where P is the strength of the electric source, ω the angular frequency, $H_0^{(1)}$ the Hankel function of zero order and of the first kind and k_b the wavenumber in the surrounding medium.

For the inverse scattering problem we assume that the unknown object is successively illuminated by L electromagnetic excitations and

for each incident field the scattered field is measured along a contour Γ at M positions. For each excitation, the direct scattering problem may be reformulated as two coupled contrast-source integral relations: the state or observation equation (3) and the field or coupling equation (4):

$$E_l^d(\mathbf{r} \in \Gamma) = k_0^2 \int_\Omega \chi(\mathbf{r}') E_l(\mathbf{r}') G(\mathbf{r}, \mathbf{r}') \mathrm{d}\mathbf{r}', \quad (3)$$

$$E_l(\mathbf{r} \in \Omega) = E_l^{inc} + k_0^2 \int_\Omega \chi(\mathbf{r}') E_l(\mathbf{r}') G(\mathbf{r}, \mathbf{r}') \mathrm{d}\mathbf{r}', \quad (4)$$

where $\chi(\mathbf{r}) = \varepsilon_r(\mathbf{r}) - \varepsilon_{br}$ denotes the permittivity contrast which vanishes outside $\Omega \supset \Omega_o$, $G(\mathbf{r}, \mathbf{r}')$ is the two-dimensional homogeneous space Green's function and k_0 represent the wavenumber in the vacuum. For the sake of simplicity, the equations (3) and (4) are rewritten in operator notation as:

$$E_l^d = \mathbf{G}_\Gamma \chi E_l, \quad (5)$$

$$E_l = E_l^{inc} + \mathbf{G}_\Omega \chi E_l. \quad (6)$$

3. MODIFIED GRADIENT METHOD

The inverse scattering problem consists in finding the function χ in the investigated area Ω from the measured scattered field. In order to solve this problem, a modified gradient method [10] is considered. This method consists to construct two sequences related to the contrast $\{\chi_n\}$ and to the total field $\{E_{l,n}\}$ using the following recursive relations:

$$\chi_n = \chi_{n-1} + \beta_n d_n, \quad (7)$$

$$E_{l,n} = E_{l,n-1} + \alpha_{l,n} v_{l,n}, \quad (8)$$

where d_n and $v_{l,n}$ are search directions with respect to χ_n and $E_{l,n}$, respectively. The scalar coefficients β_n and $\alpha_{l,n}$ are chosen at each iteration step n such that they minimize the normalized cost functional $F_n(\chi_n, E_{l,n})$ given by:

$$F_n(\chi_n, E_{l,n}) = W_\Omega \sum_{l=1}^{L} ||h_{l,n}^{(1)}||_\Omega^2 + W_\Gamma \sum_{l=1}^{L} ||h_{l,n}^{(2)}||_\Gamma^2, \quad (9)$$

where W_Ω and W_Γ are the normalizing coefficients defined as:

$$W_\Omega = \frac{1}{\sum_{l=1}^{L} ||E_l^{inc}||_\Omega^2}, \qquad W_\Gamma = \frac{1}{\sum_{l=1}^{L} ||E_l^d||_\Gamma^2}. \quad (10)$$

The functions $h_{l,n}^{(1)}$ and $h_{l,n}^{(2)}$ are the residual errors in the field equation and in the observation equation, respectively. They are defined as follows:

$$h_{l,n}^{(1)} = E_l^{inc} - E_{l,n-1} + \mathbf{G}_\Omega \chi_n E_{l,n}, \tag{11}$$

$$h_{l,n}^{(2)} = E_l^d - \mathbf{G}_\Gamma \chi_n E_{l,n}. \tag{12}$$

Dealing with the reconstruction of complex objects, it appears wise to consider separately the real and imaginary part in the MGM algorithm scheme. Therefore, in order to obtain an efficient implementation of the MGM, the complex contrast function is redefined as follows:

$$\chi_n = \xi_n + i\eta_n - \varepsilon_{br}, \tag{13}$$

where ξ_n and η_n are two real auxiliary functions. The recursive relation with respect to the complex function χ_n reads:

$$\xi_n = \xi_{n-1} + \beta_n^\xi d_n^\xi, \tag{14}$$

$$\eta_n = \eta_{n-1} + \beta_n^\eta d_n^\eta, \tag{15}$$

where all quantities are real. The minimization of F_n is accomplished using the Polak-Ribière conjugate gradient method [14]. The updating directions d_n^ξ and d_n^η are the standard Polak-Ribière conjugate gradient directions:

$$d_n^\xi = g_n^\xi + \gamma_n^\xi d_{n-1}^\xi \quad \text{with} \quad \gamma_n^\xi = \frac{\left\langle g_n^\xi | g_n^\xi - g_{n-1}^\xi \right\rangle_\Omega}{||g_{n-1}^\xi||_\Omega^2}, \tag{16}$$

$$d_n^\eta = g_n^\eta + \gamma_n^\eta d_{n-1}^\eta \quad \text{with} \quad \gamma_n^\eta = \frac{\langle g_n^\eta | g_n^\eta - g_{n-1}^\eta \rangle_\Omega}{||g_{n-1}^\eta||_\Omega^2}, \tag{17}$$

where $\langle . | . \rangle_D$ represent the inner product defined on $L^2(D)$ and g_n^ξ and g_n^η are the gradients of the cost functional $F_n(\xi_n, \eta_n, E_{l,n})$ with respect to ξ_n and η_n, respectively, evaluated at the $(n-1)^{\text{th}}$ step assuming that the total field inside the scattering domain does not change. These gradients are given by:

$$g_n^\xi = \text{Re}\left[W_\Omega \sum_{l=1}^{L} \bar{E}_{l,n-1} \mathbf{G}_\Omega^\dagger h_{l,n-1}^{(1)} - W_\Gamma \sum_{l=1}^{L} \bar{E}_{l,n-1} \mathbf{G}_\Gamma^\dagger h_{l,n-1}^{(2)} \right], \tag{18}$$

$$g_n^\eta = \text{Im}\left[W_\Omega \sum_{l=1}^{L} \bar{E}_{l,n-1} \mathbf{G}_\Omega^\dagger h_{l,n-1}^{(1)} - W_\Gamma \sum_{l=1}^{L} \bar{E}_{l,n-1} \mathbf{G}_\Gamma^\dagger h_{l,n-1}^{(2)} \right], \tag{19}$$

where $\bar{E}$ denotes the complex conjugate of the field E; while $\mathbf{G}_\Omega^\dagger$ and $\mathbf{G}_\Gamma^\dagger$ are the adjoint operators of $\mathbf{G}_\Omega$ and $\mathbf{G}_\Gamma$, respectively.

The search direction for the total field is also taken as the Polak-Ribière conjugate gradient direction:

$$v_{l,n} = g_{l,n}^v + \gamma_{l,n}^v v_{l,n-1} \quad \text{with} \quad \gamma_{l,n}^v = \frac{\left\langle g_{l,n}^v | g_{l,n}^v - g_{l,n-1}^v \right\rangle_\Omega}{||g_{l,n-1}^v||_\Omega^2}, \tag{20}$$

where $g_{l,n}^v$ is the gradient of the cost functional $F_n(\xi_n, \eta_n, E_{l,n})$ with respect to $E_{l,n}$ evaluated at the $(n-1)^{\text{th}}$ step assuming that the object functions ξ_n and η_n do not change. This gradient is given by:

$$g_{l,n}^v = W_\Omega \left[\bar{\chi}_{n-1} \mathbf{G}_\Omega^\dagger h_{l,n-1}^{(1)} - h_{l,n-1}^{(1)} \right] - W_\Gamma \bar{\chi}_{n-1} \mathbf{G}_\Gamma^\dagger h_{l,n-1}^{(2)}. \tag{21}$$

4. BAYESIAN INTERPRETATION OF THE JOINT ESTIMATION

In this contribution, in order to solve the inverse problem, the joint estimation of the contrast χ and the total field E was considered through an extended modified gradient method. To improve the solution, *a priori* knowledge is added. A Bayesian estimation framework [6] can be taken into account in order to define a regularized solution.

In what follows, an additive zero mean white Gaussian and centered circular noise is assumed to model the errors on the measurement. Moreover, in the attempt to reconstruct images constituted by homogeneous area, the *a priori* knowledge of the object can be modelled by the following probability law:

$$p(\chi) \propto \exp(-U(\chi)), \tag{22}$$

where $U(\chi)$ is the energy function.

Taking into account the previous consideration, the solution of the coupled equations can be defined as the joint maximum *a posteriori* of χ and E:

$$(\chi, E)_{MAP} = argmax_{(\chi,E)} p(\chi, E|E^d), \tag{23}$$

where, from the Bayes' rule, $p(\chi, E|E^d)$ is given by:

$$p(\chi, E|E^d) = \frac{p(E^d|\chi, E)p(E|\chi)p(\chi)}{p(E^d)}. \tag{24}$$

In this equation, the denominator $p(E^d)$ is a normalization constant. From (5) and taking into account the considered error model, the first numerator term can be written as:

$$p(E^d|\chi, E) \propto \exp\left(-\frac{1}{\sigma_b^2}||E^d - \mathbf{G}_\Gamma \chi E||^2\right). \tag{25}$$

where σ_b^2 is the noise variance. The second term $p(E|\chi)$ representing the probability density of E for a known χ is defined from (6):

$$p(E|\chi) = \delta\left(E - E^{inc} - \mathbf{G}_\Omega \chi E\right), \tag{26}$$

where δ is the Dirac distribution

The joint *a posteriori* law on χ and E is then given by:

$$p(\chi, E|E^d) \propto \exp\left(-\frac{1}{\sigma_b^2}||E^d - \mathbf{G}_\Gamma \chi||^2 - U(\chi)\right) \delta\left(E - E^{inc} - \mathbf{G}_\Omega \chi E\right). \tag{27}$$

Finally, the estimate of (χ, E) in the sense of the maximum *a posteriori* comes down to minimizing the following criterion:

$$F(\chi, E) = ||E^d - \mathbf{G}_\Gamma \chi E||^2 + U(\chi), \tag{28}$$

within the constraint:

$$E - E^{inc} - \mathbf{G}_\Omega \chi E = 0. \tag{29}$$

One can note that taking into account the Bayes' rule, it seems to be unnecessary to introduce an *a priori* model on E since the information on E is given by $p(E|\chi)$. Therefore, the criterion requires only a regularization term on χ, which corresponds to the *a priori* law $p(\chi)$. Moreover, one can note that criterion (28) is not a convex function.

5. REGULARIZED MODIFIED GRADIENT METHOD

5.1. Formulation of the Regularized MGM

As previously noted, dealing with complex object, it seems wise to consider the real and the imaginary parts separately. In this way, the general cost functional under consideration $\tilde{F}_n(\xi_n, \eta_n, E_{l,n})$ can be defined as:

$$\tilde{F}_n(\xi_n, \eta_n, E_{l,n}) = F_n(\xi_n, \eta_n, E_{l,n}) + U_n^\xi(\xi_n) + U_n^\eta(\eta_n), \tag{30}$$

where $U_n^{\xi}(\xi_n)$ and $U_n^{\eta}(\eta_n)$ are regularizing energies acting on the real and imaginary parts of the object, respectively, and $F_n(\xi_n, \eta_n, E_{l,n})$ is the previous cost functional presented in Section 3. One can note that different energies for the real and imaginary parts can be taken into account; in our case, the same energies, corresponding to the weak membrane model, have been considered.

From this formulation, the modification of the MGM algorithm appears essentially on the contrast search directions. The recursive relations for the regularized MGM are then given by:

$$\xi_n = \xi_{n-1} + \beta_n^{\xi} \tilde{d}_n^{\xi}, \tag{31}$$

$$\eta_n = \eta_{n-1} + \beta_n^{\eta} \tilde{d}_n^{\eta}, \tag{32}$$

$$E_{l,n} = E_{l,n-1} + \alpha_{l,n} v_{l,n}, \tag{33}$$

where $\tilde{d}_n^{\xi}$ and $\tilde{d}_n^{\eta}$ are the updating directions with respect to ξ_n and η_n, respectively. They are defined as follows:

$$\tilde{d}_n^{\xi} = \tilde{g}_n^{\xi} + \tilde{\gamma}_n^{\xi} \tilde{d}_{n-1}^{\xi} \quad \text{with} \quad \tilde{\gamma}_n^{\xi} = \frac{\left\langle \tilde{g}_n^{\xi} | \tilde{g}_n^{\xi} - \tilde{g}_{n-1}^{\xi} \right\rangle_{\Omega}}{||\tilde{g}_{n-1}^{\xi}||_{\Omega}^2}, \tag{34}$$

$$\tilde{d}_n^{\eta} = \tilde{g}_n^{\eta} + \tilde{\gamma}_n^{\eta} \tilde{d}_{n-1}^{\eta} \quad \text{with} \quad \tilde{\gamma}_n^{\eta} = \frac{\langle \tilde{g}_n^{\eta} | \tilde{g}_n^{\eta} - \tilde{g}_{n-1}^{\eta} \rangle_{\Omega}}{||\tilde{g}_{n-1}^{\eta}||_{\Omega}^2}, \tag{35}$$

where $\tilde{g}_n^{\xi}$ and $\tilde{g}_n^{\eta}$ are the gradients of the cost functional $\tilde{F}_n(\xi_n, \eta_n, E_{l,n})$ with respect to ξ_n and η_n, respectively. In fact, it can be easily shown that the search directions $\tilde{d}_n^{\xi}$ and $\tilde{d}_n^{\eta}$ correspond to:

$$\tilde{d}_n^{\xi} = d_n^{\xi} + \hat{d}_n^{\xi}, \tag{36}$$

$$\tilde{d}_n^{\eta} = d_n^{\eta} + \hat{d}_n^{\eta}, \tag{37}$$

where $\hat{d}^{\xi}$ and $\hat{d}^{\eta}$ are the regularizing search directions which depend on the choice of $U(t)$.

5.2. Weak Membrane Model

In this contribution, a Markovian energy corresponding to the weak membrane model [5] is proposed as regularizing term. This energy permits to take into account a local correlation between adjacent pixels and corresponds to a locally gaussian, non-stationary first-order Markovian chain with boolean line process [13]. It acts locally to smooth the signal while preserving abrupt transitions.

The weak membrane model is defined as a sum of truncated quadratic potential functions parameterized by (α, μ):

$$U(\mathbf{c}) = \rho \sum_{i=1}^{N} h_{\alpha,\mu}(c_i - c_{i-1}) \tag{38}$$

where ρ is the weighting parameter (experimentally chosen) and the functional $h_{\alpha,\mu}(.)$ defined by:

$$h_{\alpha,\mu}(t) = \begin{cases} \alpha^2 t^2 & \text{if} \quad |t| < T \\ \mu & \text{if} \quad |t| \geq T \end{cases} \qquad T = \frac{\sqrt{\mu}}{\alpha}, \tag{39}$$

involves an implicit contour process. In (38) and (39), c corresponds to either ξ or η, and α is a scale parameter which defines the dispersion of the homogeneous zone while μ fixes the *a priori* discontinuity detection threshold T. Since this functional is not differentiable at $|t| = T$, a relaxation scheme based on the graduated non convexity principle [5] was considered. The functional h is then modified as follows:

$$h_{\alpha,\mu,\zeta}(t) = \begin{cases} \alpha^2 t^2 & \text{if} \quad |t| < q \\ \mu - \dfrac{\zeta(|t| - r)^2}{2} & \text{if} \quad q \leq |t| < r, \\ \mu & \text{if} \quad |t| \geq r \end{cases} \tag{40}$$

where α is a scale parameter which defines the dispersion of the homogeneous zone while μ fixes the threshold of discontinuities $h_0 = \frac{\sqrt{2\mu}}{\alpha}$. $\zeta (\in [\zeta_0, \infty[)$ is the relaxation parameter such as $\lim_{\zeta \to \infty} h_{\alpha,\mu,\zeta}(t) = h_{\alpha,\mu}(t)$ (in practice, only some relaxations are used). Moreover, the threshold expression of r and q are $r^2 = \mu(2/\zeta + 1/\alpha^2)$ and $q = \mu/\alpha^2 r$. Figure 2 shows the weak membrane function and the relaxed scheme. The final criterion $\tilde{F}_{n,\zeta}$ is defined as:

$$\tilde{F}_{n,\zeta}(\xi_n, \eta_n, E_{l,n}) = F_n(\xi_n, \eta_n, E_{l,n}) + U^{\xi}_{n,\zeta}(\xi_n) + U^{\eta}_{n,\zeta}(\eta_n) \tag{41}$$

which is then minimized thanks to the extended MGM algorithm for a fixed ζ. The inversion is processed by relaxations of ζ (see Figure 2) — followed by a local MGM minimization. Moreover, taking into account [11], the total field is fully computed using (6) at each relaxation of ζ.

One can note that without defining the contrast function as (13) and considering a regularization scheme which acts separately on the real and imaginary parts of the object, the real and imaginary weighting parameters would finally affect both object parts, making their choice difficult and finally impossible.

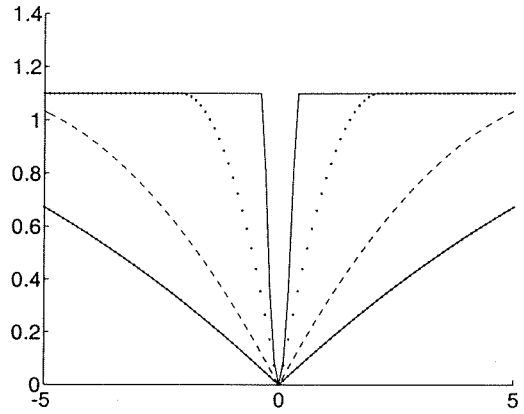

Figure 2. Relaxed weak membrane energy for $\mu = 1.10$, $\alpha = 3$ and $\zeta = 0.0125$ ('·-'), 0.05 ('- -'), 0.5 ('··') and ∞ ('-').

6. REAL DATA

6.1. Experimental Setup

The considered experimental setup (Figure 3), from Institut Fresnel (Marseille, France), is described in [3, 4]. A dielectric or metallic homogeneous object is successively irradiated by $L = 36$ different sources evenly distributed around the object. The TM polarized incident fields, E_l^{inc} $(l = 1, \ldots, L)$, are modelled in the investigating domain by a linearly polarized isotropic cylindrical wave as defined in (2). The scattered field for each irradiation E_l^d is measured for $M = 72$ different locations evenly distributed around the object. However, due to physical limitations, there is a blind zone of 120° (in dashed line on Figure 3) such that the scattered field is measured for 49 out of the 72 receiver angles.

In the following, some reconstructions using the proposed algorithm and the experimental data are presented. An initial guess based on a back propagation method, as described in [3], has been considered to initialize the reconstructions. Moreover, on each figure, the results are presented using gray level maps with values greater than the unity for the dielectric objects and with non negative normalized values for the metallic target, because for such impenetrable objects only the contour is of interest — the conductivity estimated level being less important.

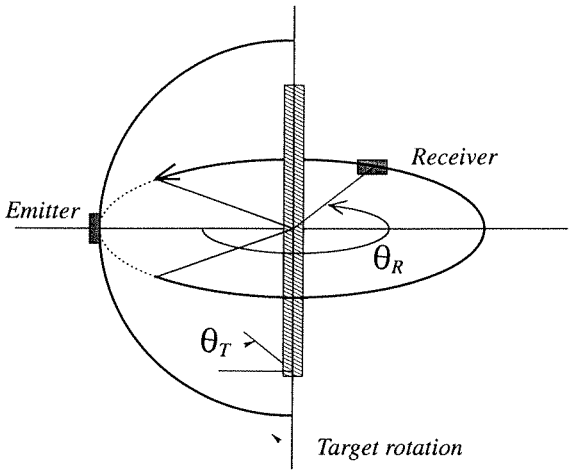

Figure 3. The experimental setup geometry used for validating the inverse algorithm. θ_R denotes the angle of receiving antenna while θ_T represents the angle of the emitting antenna.

6.2. Dielectric Targets

6.2.1. Single Dielectric Object

A single non-centered dielectric cylinder with circular cross-section of radius 1.5 cm is considered. The relative permittivity of this target was estimated at $\varepsilon_r = 3 \pm 0.3$ by an experimental method [3]. In this contribution, the data associated with the so called dielTM_dec_8f.exp file are considered, and the operating frequency corresponding to 4 GHz is used. For this frequency, a search domain of 6.5 cm (along the x-axis) $\times$ 6.5 cm (along the y-axis), discretized into 32 $\times$ 32 cells and centered at ($x = -0.28$ cm, $y = -3$ cm) has been considered. Figure 4 presents the simulated object under consideration for the previous search domain, the reconstruction obtained after 150 iterations without regularization and the reconstruction obtained using the regularized MGM after 150 iterations (5 sequences composed of 25 iterations for the local minimization). The permittivity level at 4 GHz is $\varepsilon_r = 5.47$ in the non regularized case and $\varepsilon_r = 4.17$ in the regularized case. Figure 5 show a cross-section, along the x-axis, at $y = -3$ cm, of the results which permits to compare the actual relative permittivity with the reconstructed one.

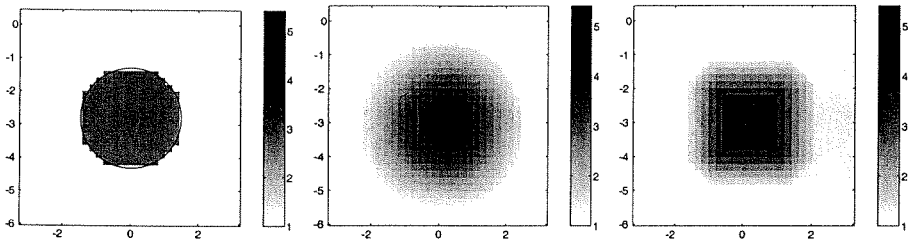

(a) (b) (c)

Figure 4. Reconstruction of the dielectric object at 4 GHz after 150 iterations. (a) Simulated 6.5 cm × 6.5 cm search domain centered at ($x = -0.28$ cm, $y = -3$ cm) and discretized into 32 × 32 cells. The solid line represents the shape of the non discretized object. (b) Reconstruction obtained without regularization. (c) Reconstruction obtained with regularization.

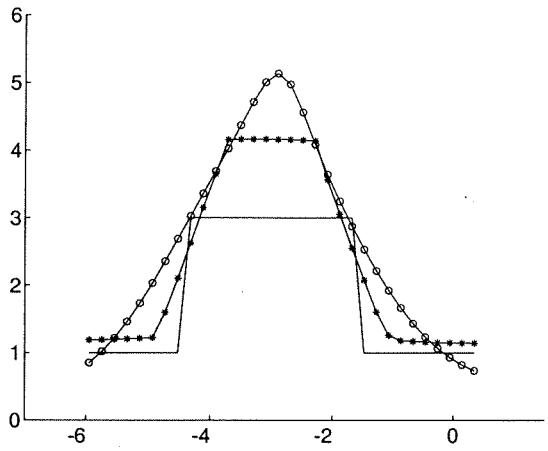

Figure 5. Cross-sectional of the simulated object (solid line) and the reconstructions obtained at 4 GHz without regularization (dotted line) and with regularization (stared line).

6.2.2. Two Dielectric Objects

Here, a dielectric target made up of twin cylinders with circular cross-section of radius 1.5 cm is considered. The relative permittivity of this target was estimated at $\varepsilon_r = 3 \pm 0.3$. The data associated with the so called twodielTM_8f.exp file for 4 GHz and 7 GHz are considered. For both frequencies, a rectangular search domain of

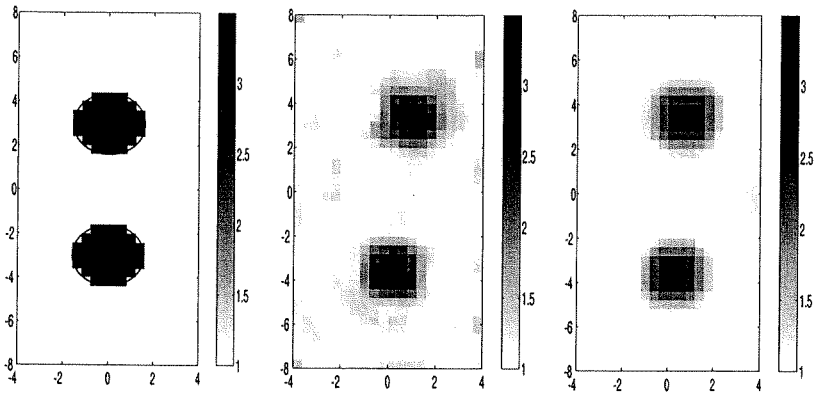

(a) (b) (c)

Figure 6. Reconstruction obtained after 175 iterations of the two dielectric objects at 4 GHz. (a) Simulated 8 cm × 16 cm search domain centered at (x = 0 cm, y = 0 cm) and discretized into 20 × 40 cells. The solid line represents the shape of the non discretized object. (b) Reconstruction obtained without regularization. (c) Reconstruction obtained with regularization.

8 cm (along the x-axis) × 16 cm (along the y-axis) was discretized into 20 × 40 cells and centered at (x = 0 cm, y = 0 cm). Figures 6 and 7 show the simulated object for the previous search domain, the reconstruction obtained after 175 iterations without regularization and the reconstruction obtained after 175 iterations (5 sequences composed of 35 iterations for the local minimization) using the regularized MGM at 4 GHz and 7 GHz, respectively. The permittivity level at 4 GHz is $\varepsilon_r = 3.49$ and $\varepsilon_r = 3.56$ at 7 GHz in the nonregularized case and $\varepsilon_r = 2.54$ at 4 GHz and $\varepsilon_r = 2.46$ at 7 GHz in the regularized one. Moreover, on can note on the obtained reconstruction a slight shift of the center of each cylinders. This shift is within the experimental margin.

6.3. Metallic Targets

6.3.1. Rectangular Metallic Object

The metallic target is a centered filled cylinder with rectangular cross-section of (1.27 × 2.54) cm^2. The experimental data correspond to the so-called rectTM_cent.exp file for 8 GHZ and 16 GHz. The search domain is a 3.6 cm × 5.4 cm area discretized into 20 × 30 cells and centered at (x = −0.5 cm, y = −0.75 cm). Figures 8 and 9 show

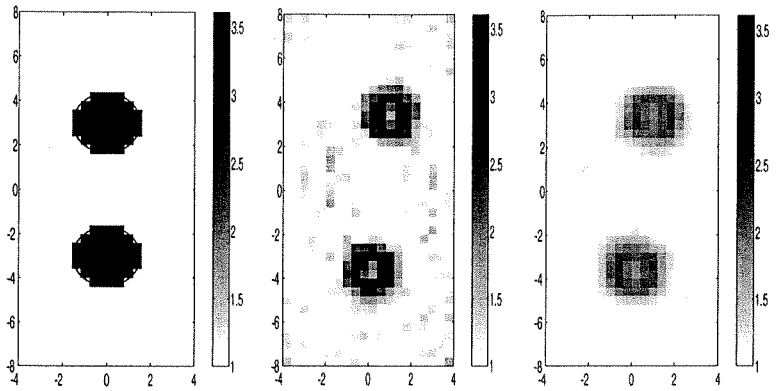

(a) (b) (c)

Figure 7. Reconstruction obtained after 175 iterations o the two dielectric objects at 7 GHz. (a) Simulated 8 cm × 16 cm search domain centered at ($x = 0$ cm, $y = 0$ cm) and discretized into 20 × 40 cells. The solid line represents the shape of the non discretized object. (b) Reconstruction obtained without regularization. (c) Reconstruction obtained with regularization.

the simulated search domain, the reconstructions obtained after 100 iterations without regularization and the results obtained after 100 iterations (5 sequences composed of 20 iterations corresponding to the local minimization) using the regularized MGM. The maximum conductivity at 8 GHz is $\sigma = 3.45$ S/m and $\sigma = 3.31$ S/m at 16 GHz in the non regularized case. In the regularized case, the maximum conductivity at 8 GHz is $\sigma = 0.85$ S/m and $\sigma = 0.31$ S/m at 16 GHz.

6.3.2. "U-shaped" Object

In this part, a "U-shaped" metallic cylinder defined within a $8 \times 5\,\text{cm}^2$ rectangle is considered. The corresponding experimental data are the so called uTM_shaped.exp file for 4 GHz and 16 GHz. The considered centered search domain is a 15 cm × 12 cm centered area discretized into 50 × 40 cells. Figures 10 and 11 show the simulated discretized search domain, the reconstructions obtained without regularization and the results obtained considering the regularized MGM for 150 iterations (5 sequences composed by 30 iterations for the local minimization). The maximum conductivity at 4 GHz is $\sigma = 4.59$ S/m and $\sigma = 1.84$ S/m at 16 GHz in the non regularized case. In the regularized case, the maximum conductivity at 4 GHz is $\sigma = 1.73$ S/m and $\sigma = 0.16$ S/m at 16 GHz.

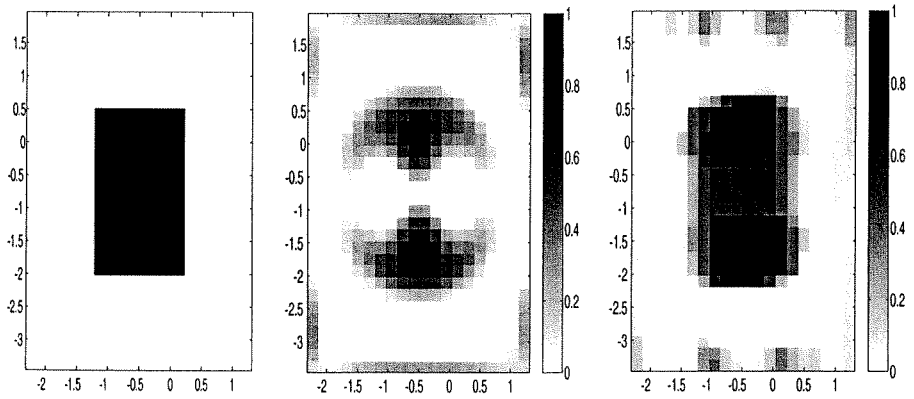

(a) (b) (c)

Figure 8. Reconstruction of the metallic target at 8 GHz after 100 iterations. Gray scale level of the (a) Simulated 3.6 $\times 5.4\,\mathrm{cm}^2$ search domain centered at ($x = -05\,\mathrm{cm}$, $y = -0.75\,\mathrm{cm}$) and discretized into 20×30 cells, (b) reconstructed target without regularization and (c) reconstruction obtained using the regularized MGM.

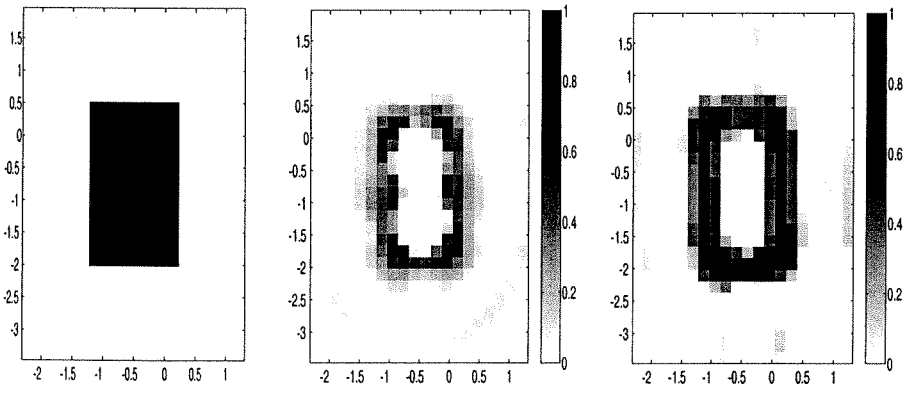

(a) (b) (c)

Figure 9. Reconstruction of the metallic target at 16 GHz after 100 iterations. Gray scale level of the (a) Simulated 3.6 $\times 5.4\,\mathrm{cm}^2$ search domain centered at ($x = -05\,\mathrm{cm}$, $y = -0.75\,\mathrm{cm}$) and discretized into 20×30 cells, (b) reconstructed target without regularization and (c) reconstruction obtained using the regularized MGM.

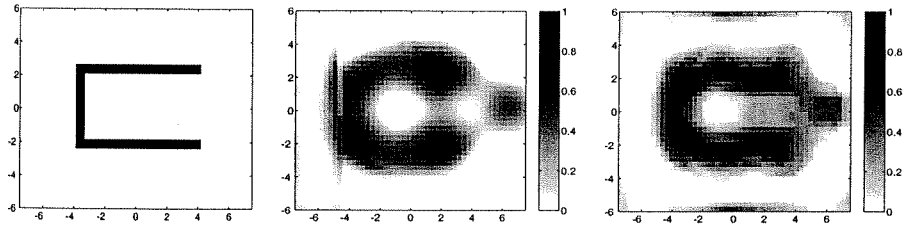

(a) (b) (c)

Figure 10. Reconstruction of the "U-shaped" metallic target at 4 GHz after 150 iterations. Gray scale level of the (a) simulated 15 cm × 12 cm centered search domain discretized into 50 × 40 cells, (b) reconstructed target without regularization and (c) reconstruction obtained using the regularized MGM.

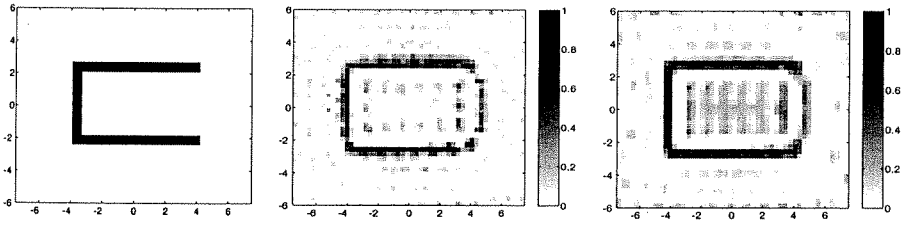

(a) (b) (c)

Figure 11. Reconstruction of the "U-shaped" metallic target at 16 GHz after 150 iterations. Gray scale level of the (a) simulated 15 cm × 12 cm centered search domain discretized into 50 × 40 cells, (b) reconstructed target without regularization and (c) reconstruction obtained using the regularized MGM.

7. CONCLUSION

In this contribution, a modification of the modified gradient algorithm was proposed in order to take into account separately the real and imaginary part of the contrast function. This algorithm has been developed in order to efficiently implement a Markovian regularization based on the weak membrane model. The proposed algorithm was tested against experimental data and the results show the improvement when considering the proposed regularized MGM. As the real data have been processed at different frequencies, future work could extend the

proposed algorithm to a multi-frequency approach. Moreover, taking into account recent works on a multiplicative TV regularization [1], a multiplicative approach of the proposed regularization method could leads to suppress the experimentally chosen weighting parameter.

REFERENCES

1. Abubakar, A. and P. M. van den Berg, "Total variation as a multiplicative constraint for solving inverse problems," *IEEE Transactions on Image Processing*, Vol. 10, No. 9, 1384–1392, 2001.
2. Baussard, A., D. Prémel, and O. Venard, "A Bayesian approach for solving inverse scattering from microwave laboratory-controlled data," *Inverse Problems*, Vol. 17, No. 6, 1659–1669, 2001.
3. Belkebir, K., S. Bonnard, F. Pezin, P. Sabouroux, and M. Saillard, "Validation of 2D inverse scattering algorithms from multi-frequency experimental data," *Journal of Electromagnetic Waves and Applications*, Vol. 14, 1637–1667, 2000.
4. Belkebir, K. and M. Saillard, "Special section: Testing inversion algorithms against experimental data," *Inverse Problems*, Vol. 17, No. 6, 1565–1571, 2001.
5. Blake, A. and A. Zisserman, *Visual Reconstruction*, MIT Press, Cambridge, 1987.
6. Carfantan, H. and A. Mohammad-Djafari, *Lectures Notes in Physics*, Chapter: An overview of nonlinear diffraction tomography within the Bayesian estimation framework, Springer Verlag, 1997.
7. Chew, W. C. and Y. M. Wang, "Reconstruction of two-dimensional permittivity distribution using distorted Born iterative method," *IEEE Trans. Med. Imaging*, Vol. 9, 218–225, 1990.
8. Devaney, A. J., "Geophysical diffraction tomography," *IEEE Trans. Geosci. Remote Sensing*, Vol. 22, 3–13, 1984.
9. Joachimowicz, N., C. Pichot, and J. P. Hugonin, "Inverse scattering: An iterative numerical method for electromagnetic imaging," *IEEE Trans. Antennas Propagat.*, Vol. 39, 1742–1751, December 1991.
10. Kleinman, R. E. and P. M. van den Berg, "A modified gradient method for two-dimensional problems in tomography," *Journal of Computational and Applied Mathematics*, Vol. 42, 17–35, 1992.

11. Lambert, M., D. Lesselier, and B. J. Kooij, "The retrieval of a buried cylindrical obstacle by a constrained modified gradient method in the h-polarization case and for maxwellian materials," *Inverse Problems*, Vol. 14, 1265–1283, 1998.
12. Nikolova, M. and A. Mohammad-Djafari, "Discontinuity reconstruction from linear attenuating operators using the weak-string model," *Proceedings of European Signal Processing Conference*, Vol. 2, 1062–1065, 1994.
13. Nikolova, M., J. Idier, and A. Mohammad-Djafari, "Inversion of large-support ill-posed linear operators using a piecewise Gaussian MRF," *IEEE Trans. on Image Processing*, Vol. 7, No. 4, 571–585, 1998.
14. Press, W. H., B. P. Flannery, S. A. Teukolski, and W. T. Vetterling, *Numerical Recipes. The art of scientific computing*, Cambridge University Press, 1986.
15. Tabbara, W., B. Duchene, C. Pichot, L. Chommeloux, and N. Joachimowicz, "Diffraction tomography: Contribution to the analysis of some applications in microwave and ultrasonics," *Inverse Problems*, Vol. 4, 305–331, April 1988.
16. van den Berg, P. M. and R. E. Kleinman, "A contrast source inversion method," *Inverse Problems*, Vol. 13, 1607–1620, 1997.
17. van den Berg, P. M. and R. E. Kleinman, "A total variation enhanced modified gradient algorithm for profile reconstruction," *Inverse Problems*, Vol. 11, L5–L10, 1995.
18. Venard, O., D. Premel, and A. Mohammad-Djafari, "Eddy current tomography: A Bayesian approach with a compound weak membrane-Beta prior model," *IIIth International Workshop — Advances in Signal Processing for Non Destructive Evaluation of Materials*, Vol. 3, 155–161, Quebec, Canada, 1997.

Alexandre Baussard is currently a Ph.D. student at SATIE (Systèmes et Applications des Technologies de l'Information et de l'Energie) laboratory, Ecole Normale Supérieure de Cachan, France. His research deals with forward and inverse problems.

Kamal Belkebir was born in Algeria in 1966. He received the Ph.D. degree in Physics from the University of Paris XI (Orsay), France in 1994. He worked from 1995 to 1997 at the University of Eindhoven, the Netherlands on Post-doctoral position. He joined the Laboratoire d'Optique Electromagnétique in 1997 and he is currently "Maître de Conférences" at the University of Provence in Marseille. His research deals with both forward and inverse scattering techniques.

Denis Prémel was born in France in 1960. He received the "Agrégation de Génie Electrique" in 1986 and the Ph.D. degree in 1992 from the University of Paris XI (Orsay). He worked from 1994 to 2002 at the Ecole Normale Supérieure de Cachan on a "Maître de Conférences" position. He is currently at the DRT/DECS/SISC/LCME CEA Saclay. His research interests include inverse scattering methods applied to eddy current non destructive evaluation.